

SCIENTIFIC REPORTS



OPEN

Anodically Grown Titania Nanotube Induced Cytotoxicity has Genotoxic Origins

Received: 21 September 2016

Accepted: 30 December 2016

Published: 06 February 2017

M. Sheikh Mohamed¹, Aida Torabi², Maggie Paulose², D. Sakthi Kumar¹ & Oomman K. Varghese²

Nanoarchitectures of titania (TiO₂) have been widely investigated for a number of medical applications including implants and drug delivery. Although titania is extensively used in the food, drug and cosmetic industries, biocompatibility of nanoscale titania is still under careful scrutiny due to the conflicting reports on its interaction with cellular matter. For an accurate insight, we performed *in vitro* studies on the response of human dermal fibroblast cells toward pristine titania nanotubes fabricated by anodic oxidation. The nanotubes at low concentrations were seen to induce toxicity to the cells, whereas at higher concentrations the cell vitality remained on par with controls. Further investigations revealed an increase in the G₀ phase cell population depicting that majority of cells were in the resting rather than active phase. Though the mitochondrial set-up did not exhibit any signs of stress, significantly enhanced reactive oxygen species production in the nuclear compartment was noted. The TiO₂ nanotubes were believed to have gained access to the nuclear machinery and caused increased stress leading to genotoxicity. This interesting property of the nanotubes could be utilized to kill cancer cells, especially if the nanotubes are functionalized for a specific target, thus eliminating the need for any chemotherapeutic agents.

Recent advances in the synthesis and development of nanomaterials (NMs) of diverse origins, structures and properties have immensely impacted various fields ranging from consumer electronics to medical diagnosis and therapy. At such a rapid pace of NMs' intrusion into virtually every aspect of life, the concern over their possible adverse or deleterious effects on life forms has become a major topic of discussion¹. As the NMs differ widely with respect to their physicochemical parameters such as size, shape and elemental constituents, analysis of their toxicity involves complex challenges². In addition, cell culture conditions, cell age and cell density can also influence the toxicity of the nanostructures³. Research so far has revealed different modes of NMs induced toxicity including the induction of oxidative stress due to reactive oxygen species (ROS) generation, inflammation, genetic damage and arresting of cell division, all culminating in cell death⁴⁻⁷. Different routes of exposure have also been shown to cause NM accumulation in major organs and induce toxicity⁸⁻¹⁴.

Among the various kinds of NMs currently in focus, the nanotubes (NTs) have been proven most useful for many applications due to their architecture derived unique functionalities^{15,16}. The tubular shape, inner and outer surfaces and the nanoscale wall, all provide them distinct advantages over other nanoarchitectures. A prerequisite for their *in vivo* use is an in-depth understanding on their toxicological effects. The toxicity of nanoparticles of iron oxide, gold and cadmium chalcogenides, were investigated but the studies were limited to nearly isotropic particles¹⁷⁻¹⁹ (*i.e.*, with a low aspect ratio compared to fibers). Most studies on the bio-applications and toxicity have so far almost been exclusively focused on carbon based NTs²⁰⁻²⁶. Similar studies were also reported on other one dimensional materials including silver nanowires (NWs), silicon NWs and germanium-imogolite nanotubes²⁷⁻³⁰. Although there were some attempts (discussed later), the toxicity of oxide nanotubes³¹ such as titanium dioxide (TiO₂) NTs has not been addressed in detail. We note that titanium and its alloys are currently the most widely employed materials for dental and orthopedic implants owing to their non-toxicity and biocompatibility along with commendable mechanical properties and corrosion resistance^{32,33}.

¹Bio Nano Electronics Research Centre, Graduate School of Interdisciplinary New Science, Toyo University, Kawagoe, 350-8585 Japan. ²Nanomaterials and Devices Laboratory, Department of Physics, University of Houston, Houston, Texas 77204, USA. Correspondence and requests for materials should be addressed to D.S.K. (email: sakthi@toyo.jp) or O.K.V. (email: okvarghese@uh.edu)

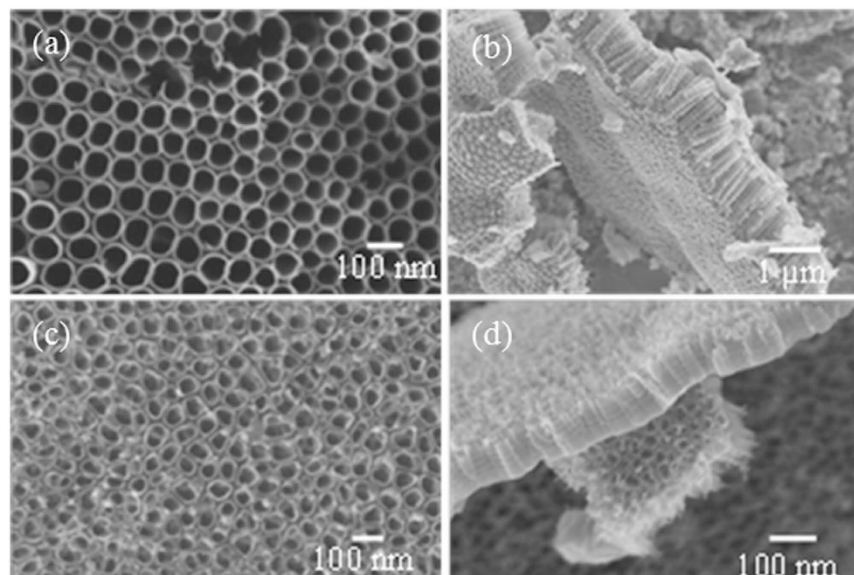


Figure 1. SEM images of TiO₂ nanotube array films separated from substrates. (a) Top and (b) lateral views of the nanotubes fabricated using the EG/NH₄F electrolyte. (c) and (d) show the images of the corresponding regions in films grown in the water/HF electrolyte.

While titania nanotubes can be fabricated by a number of physical, chemical and electrochemical methods, the self-assembled nanotube arrays grown by anodic oxidation has received incredible attention due to the ease in fabrication as well as the exceptional structural, electrical, thermal and optical properties exhibited by them^{34–36}. These nanotubes find potential use in *in-vivo* applications also. In a number of studies on the cell response to TiO₂ nanotubes, nanosize effects were demonstrated for a variety of cells^{37,38}. It was reported that the surface topography of nanoscale TiO₂ strongly affected the proliferation, migration, and differentiation of mesenchymal stem cells and hematopoietic stem cells, as well as the behavior of osteoblasts and osteoclasts³⁹ which prevailed even after coating the nanotubes with an alloy⁴⁰. It was established that the geometric factors of nanotubes greatly influenced cell vitality. We note that most of the so called ‘biocompatible materials’ including titanium and its alloys, have shown to instigate inflammatory cell recruitment, granulation tissue formation, foreign body reaction, fibrosis and other related biological events^{41,42}. Such unwarranted events may lead to poor skin–material integration, which is one of the major causes for transcatheter implantable devices’ rejection and undesired side effects^{43–45}. Therefore, it is of extreme importance that nanomaterials, regardless of their physicochemical characteristics, be thoroughly investigated under *in vitro* and *in vivo* conditions prior to human and environmental exposure. Herein, we discuss the results of our comprehensive study on the anodically grown TiO₂ nanotubes for their compatibility towards human dermal fibroblasts. We used a variety of assays ranging from cell-vitality to mitochondrial, cytoskeletal and nuclear integrity. Our investigations revealed for the first time the titania nanotube induced cyto/genotoxicity.

Results and Discussion

TiO₂ Nanotubes. As discussed in detail in Materials and Methods, we used titania nanotube arrays anodically grown in hydrofluoric acid (HF)/water and ethylene glycol (EG)/Ammonium fluoride (NH₄F) electrolytes for the study. Fig. 1 shows the field emission scanning electron microscope (SEM; LEO 1525) images of the as-fabricated nanotube arrays. The nanotubes grown in HF/H₂O electrolyte had an average length of 146 nm and pore diameter 35 nm and those grown in EG/NH₄F electrolyte had these dimensions 970 nm and 70 nm respectively. These nanotube arrays, after heat treatment and detachment from the substrate, were sonicated in water to obtain dispersed individual nanotubes for further experiments. The transmission electron microscope (TEM; JEOL JEM-2100) images of these dispersed nanotubes are shown in Fig. 2. It is evident from the TEM images that nanotubes were broken during detachment and were of similar length (~150 nm) regardless of the fabrication conditions. The NTs were devoid of any metal substrate elements as NT array films were detached electrochemically from the substrates (see Materials and Methods).

The anodically grown NTs are generally amorphous upon formation and are known to crystallize at ~280 °C with anatase phase formed in the NT walls^{46,47}. The selected area diffraction pattern and the lattice image showing polycrystalline anatase phase present in the wall of an NT prepared using EG/NH₄F electrolyte and heat treated at 530 °C are given in Supporting Information Fig. S1. The HF and EG based NTs used in the present study were crystallized by heat treating at 500 and 450 °C respectively.

Cytotoxicity Analyses. Nanotubes generally share morphological similarities with asbestos fibrils, which are linked to progressive fibrotic ailments⁴⁸. On this basis we explored the acute cytotoxicity of NTs on human dermal fibroblast cells (HDAF). The effect of NTs on the proliferation and metabolic status of the cells was first investigated by alamar blue assay. The NTs fabricated by both aqueous and organic electrolytes were slightly toxic

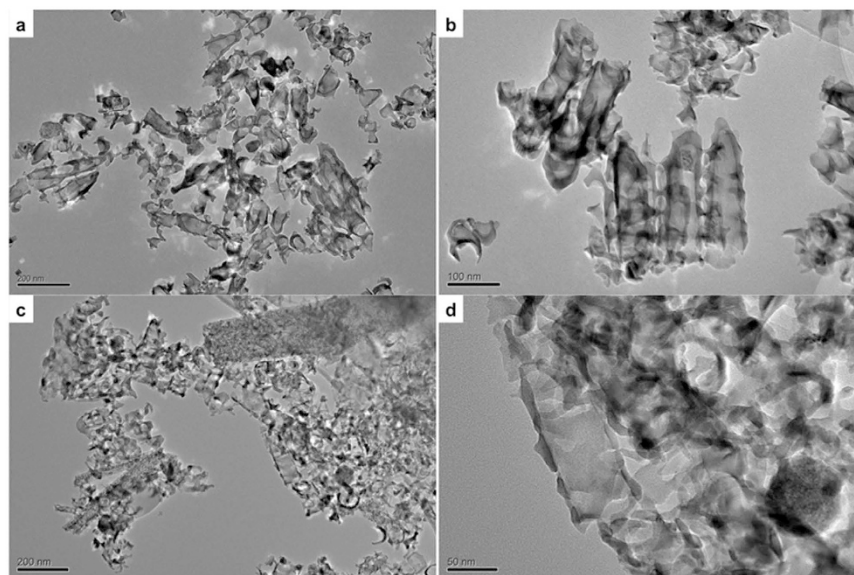


Figure 2. TEM micrographs of TiO₂ nanotubes. (a) Low magnification and (b) high magnification images of ethylene glycol (organic) electrolyte fabricated TiO₂ nanotubes. (c) Low magnification and (d) high magnification images of HF/H₂O (aqueous) electrolyte fabricated TiO₂ nanotubes.

at lower concentrations (0.05, 0.1 and 0.25 mg/mL) when compared to the higher concentrations (0.5–1.0 mg/mL) after the incubation period of 72 h. In the case of samples fabricated using EG electrolyte, the viability reduced to 60.37, 62.26 and 68.86% for 0.05, 0.1 and 0.25 mg/mL NTs treated set, respectively (Fig. 3a). Higher concentrations i.e., 0.5, 0.75 and 1.0 mg/mL, showed 78.77, 78.94 and 88.22% viabilities, respectively. Although the nanotubes fabricated by HF/H₂O electrolyte were significantly shorter (by a factor of ~6) originally, similar results were obtained from these nanotubes also (see Supporting Information Fig. S2). Nonetheless, as mentioned earlier, the dimensions of nanotubes prepared in both the electrolytes became similar after sonication. It is reasonable to believe that the similarity in the toxic nature of both types of nanotubes arises from their comparable dimensions. The study also confirmed that the nanotube pedigree had no apparent role in determining the toxicity. For these reasons, we used the samples prepared using EG/NH₄F electrolyte for all subsequent studies.

The broken NTs were found to be aggregated and difficult to disperse by sonication. Post sonication, uneven polydisperse size distribution in solutions was evident from Fig. 2a. This observation was similar to earlier studies on carbon nanotubes, where the length and morphology of the carbon nanotubes were distorted after sonication^{49,50}. The extent of aggregation increased when NTs were added to the cell culture media which could likely have prevented cellular cytosol from being exposed to individual NTs at higher concentrations. It is worth mentioning that the NTs were bare and not surface functionalized with biocompatible/surfactant coating, which not only enhances the compatibility of a material but also renders significant and uniform dispersion of the nanomaterial under investigation. Due to the bare nature of NTs, exposure to cell culture medium (containing serum and various proteins) induces aggregation and formation of large clusters that cannot be efficiently endocytosed by cells and therefore may not have shown toxicity. Whereas at lower concentrations, the clusters are expected to be within the endocytosis limit, leading to relatively higher uptake by cells facilitating interaction with intracellular components. Though the dosing metric is considered to be a common way to assess viability, the method is complicated because very little is known about how the aggregation behavior of the NTs affects the dosage/concentration-based toxicity. TiO₂ nanoparticles and nanotubes tend to aggregate easily in solution when not surface modified. Such aggregation behavior was reported in a few uptake and localization studies^{51–54}. Though several studies were reported on toxicity analysis of TiO₂ NTs, not much was discussed about the dosage-based aggregation of the NTs. In most of the reported studies, contradictory results were presented with some finding NTs as highly biocompatible, while some others observing toxicity in them⁵⁵. TiO₂ nanomaterials, especially the architectures with high aspect ratio such as NTs, tend to aggregate in solution. This characteristic made preparation of the dosing solutions in this study difficult because the conventional dispersion methods such as sonication provided only polydispersed solutions, which contained a mixture of individual nanotubes, nanotube aggregates, and particle debris that might have contributed to the interesting results presented here.

We point out that the nanotubes synthesized with aqueous as well as organic electrolytes, showed a similar toxicity profile, i.e., lower viability at lower concentration and higher viabilities at higher concentrations. The TEM images clearly display the fractured forms of nanotubes (Fig. 2). Though both nanotube groups differed in their structural dimensions immediately after synthesis, their morphological features became similar on sonication. We did not see any distinct difference in the cytotoxicity profiles of amorphous and polycrystalline nanotubes for a given nanotube concentration. Furthermore, as the metal substrate elements were completely removed from the nanotubes during detachment, their role in the recorded toxicity could be completely ignored. Therefore, the observed interesting cytotoxicity profile could be correlatively attributed to the size and dimensions of the test

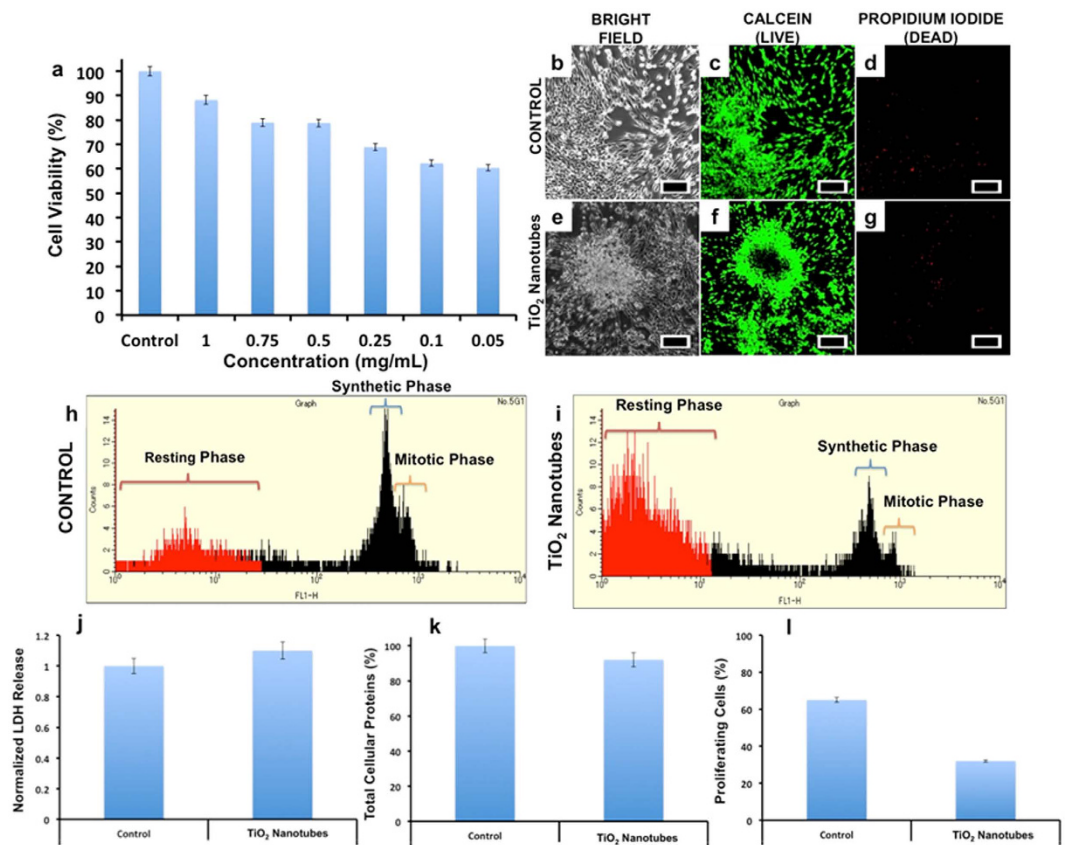


Figure 3. Cellular toxicity analysis for the effects of TiO₂ nanotubes on human dermal fibroblasts. The alamar blue assisted assay revealed a dose independent viability chart, with viability decreasing with decrease in concentration (a). Though an overall maximum viability remained at approximately 60%. (Columns, means of three independent experiments; bars \pm SD). The live dead analysis (b–g) revealed a generally live cell population in the NTs treated group (e–g) which could be correlated to the residual esterase even in the cells undergoing apoptosis (f) (scale bar represents 500 μ m). In the cell cycle analysis a predominant synthetic and mitotic phase was observed with the control cells (h), however in the NTs group a prominent resting phase was observed (i). The LDH release was found to be insignificant in treatment group when compared to control (j); The TCP expression were found to be unaffected (k) whereas the number of proliferating cells in the treatment group dropped by half when compared to control (l).

materials. The aggregation behavior was visible through microscope as well as with naked eye. The large clusters were seen to be floating in the media or attached to the cell/substratum. Therefore, it was concluded that the larger aggregates remained ineffective while the smaller aggregates or individual broken NTs specifically gained access to the cellular interior and exerted the effects observed thereof.

To assess the possible reasons for the observed toxicity of NTs based on alamar blue analysis, 0.05 mg/mL of the nanomaterial was used for all further experiments. Fluorometric live/dead cell viability and fluorometric cell cycle analysis were assayed. Using the cell viability assay that stains individual cells and measures the number of live versus dead population, it could be observed that most cells exhibited esterase staining, depicting viability (Fig. 3c,f). With alamar blue based cytotoxicity analysis, we found that nearly 40% of cell population was dead when exposed to 0.05 mg/mL of NTs after 72 h. However, with live/dead staining, almost all the cells exhibited bright green fluorescence, which we believe is from the residual esterase in the cells. It could be seen that the cells were aggregated with reduced cellular volume depicting of stress conditions (Fig. 3e), which eventually culminates in cell death. Very few cells in treatment group exhibited propidium iodide (PI) staining (Fig. 3g) which confirms that the major mode of cell-death is via the apoptotic pathway rather than necrotic. To understand whether NTs could disrupt the cell cycle progression, we analyzed the cell cycle phases of the control and treatment groups. Control group cells (Fig. 3h) were predominantly seen in synthetic and mitotic phase (S and M phase), whereas very few cells were seen in resting phase (sub G₀ phase). However, with test group (Fig. 3i), we observed a clear decline of cell population in S and M phase and a relative increase in sub G₀ phase. The cells in sub G₀ phase are indicative of cells which are no longer active part of cell-cycle.

Lactate dehydrogenase (LDH) is an important cytosolic enzyme and its release is considered to be a vital tool to understand the extent of plasma membrane damage when cells are exposed to toxic substances⁵⁶. Assessing the cell membrane integrity is one of the most common ways to measure cell viability and cytotoxic effects. When tested, the NTs exposed cells exhibited a slight increase in the LDH release as compared to the control

groups (Fig. 3j); however, the release was insignificant. If correlated with live/dead analysis, the esterase activity remained active and the cells exhibited bright green fluorescence indicative of their viable status. If the plasma membrane integrity were compromised, the esterases would have leaked out, leading to meager viable fluorescence. Furthermore, in this case the PI would have gained nuclear access exhibiting necrotic signals; the results obtained with live/dead assay clearly supports the retention of plasma membrane integrity that is observed with the LDH assay.

Total cellular proteins (TCP) constitute about 35% of cell volume and their expression could be affected when cells exhibit distress signals⁵⁷. When the TCP were quantified (Fig. 3k), the amount of proteins expressed by treatment group remained very much comparable to the control group. Though a slight decrease in protein concentrations is accounted, we believe the values are insignificant and the decrease can be attributed to treated cells that are rich in resting phase rather than in synthetic phase as seen in controls.

Cell proliferation analysis kinetics is considered as an important parameter that can critically explain about the cell's metabolic behavior at a given time⁵⁸. EDU based cell proliferation assay is considered to be easy and reliable when compared to radioactive thymidine or BrDU based analysis. EDU binds to the newly actively synthesizing DNA by click chemistry. Nearly 65% of the controls exhibited EDU staining whereas only 30% of the treated cells were positive to EDU (Fig. 3l). According to the cell cycle analyses, we believe as most of the NTs treated cells were in the resting phase with less cells in S phase, the cell proliferation ability of this group was diminished.

Cytoskeletal Organization. Cytoskeletal disorganization could also lead to serious disorientation in organelle and protein transport within the cell's cytosol and could fatally affect the cell's survival⁵⁹. A major component of cellular skeleton is actin. The actins form rigid but flexible scaffolding, facilitating the mechanical stability and mobility of cells⁶⁰. Typically, cells are flat adherent to the substratum with strong peripheral F-actin staining along the cell edge, indicative of cell cortical actin fibers. The microtubules form a dense network that is uniformly distributed around the nucleus. Microtubules are mainly responsible for mobility and intracellular transport and their proper functioning is essential for the optimal metabolic output of a cell⁶¹. Compared to control cells which displayed an elaborate network of finely arranged actin fibers (Fig. 4b), cells treated with NTs exhibited F-actin thinner and less organized within the main body (Fig. 4d), however, the microtubule structures in the central and peripheral domain remained comparable with control cells (Fig. 4f,h). This result suggested a slight disorganization of the actin cytoskeleton when exposed to NTs, which could be correlated to the observations of cellular aggregation previously mentioned. This disorganization might cause a series of signal pathway disruptions, though concrete conclusions could be made only after a detailed study of downstream processes.

Vinculin, a major membrane-cytoskeletal protein, serves as focal adhesion plaque that is involved in linking integrins to the actins and is associated with cell-cell and cell-matrix junctions⁶². Vinculin disruption can cause a loss in balance within cytoskeletal organization and can lead to contact inhibition between cells and the extra cellular matrix. When investigated, the vinculin immunomapping remained same for the control and treated group (Fig. 4j,l) depicting more or less proper cytoskeletal organization.

We investigated the expression of total focal adhesion kinase (FAK) proteins that work primarily as signal-mediating molecules that direct actin based signaling pathway⁶³. FAK disruption is known to affect cellular homeostasis. When quantified, the FAK levels of the treatment group were slightly decreased as compared to the control group (Fig. 4m). This approximately 8% decrease can be attributed to the actin disorganization that was previously observed. Though a slight modification in actin and FAK levels were noted, the cytoskeletal integrity remained comparable to the control groups. Earlier, single wall carbon nanotubes were shown to cause disorientation and bundling in actins *in vitro* leading to chronic changes in cell behavior without any observed acute toxicity⁶⁴. We believe that the observed slight actin re-modeling arose from the shape-effect of the NTs rather than their intrinsic nature bound toxicity

Mitochondrial Health. Earlier reports have emphasized the role played by oxidative stress in nanoparticle toxicity that causes serious oxidative damage to proteins and deoxyribonucleic acid (DNA)¹. To establish the role of oxidative stress as a decisive factor in NT induced toxicity, ROS tracer based studies were performed. Previous studies proved a direct link between the ROS production in cells and tissues upon exposure to titania based nanostructures⁶⁵. Untreated cells were used as standards to calculate the extent of ROS production by measuring the percentage of cells with increased fluorescence (directly corresponding to the ROS production) intensity. The analysis showed slight superoxide production in cellular cytosol, treated with 0.05 mg/mL of NTs and highly elevated levels of ROS in the nuclear compartment (Fig. 5d). As one could visualize, a dramatic increase (by 8-fold) of ROS generation could be seen in the cells that were exposed to the NTs (Fig. 5e).

Further, we investigated the mitochondrial health, as the main cause of mitochondrial dysfunction arises from ROS production and subsequent oxidative stress. Increased oxidative stress can lead to transitional pore formation in mitochondrial membrane resulting in distorted mitochondrial geometry and function⁶⁶. The discrete calcein and mitochondrial staining in the treatment group (Fig. 5g,h) revealed a normal and functioning mitochondrial apparatus. The ROS produced due to NT induced oxidative stress was likely counteracted by anti-oxidant systems/or acted upon by other organelles (especially nucleus as observed from the image), thereby nullifying their deleterious effect on mitochondria (Fig. 5k,l).

Genotoxicity. Genotoxicity studies that measure DNA damage such as mutations, chromosomal damage and single/double strand breaks are important part of cancer research and risk assessment of potential carcinogens. The oxidative stress, induction of high levels of ROS in nucleus upon NT exposure can cause spontaneous damage to DNA thus arresting the cell cycle progression. It was reported by Wang *et al.* that TiO₂ NTs could gain access into nuclear region effectively⁶⁷. To analyze whether NTs could induce genotoxicity, we assessed the chromosomal

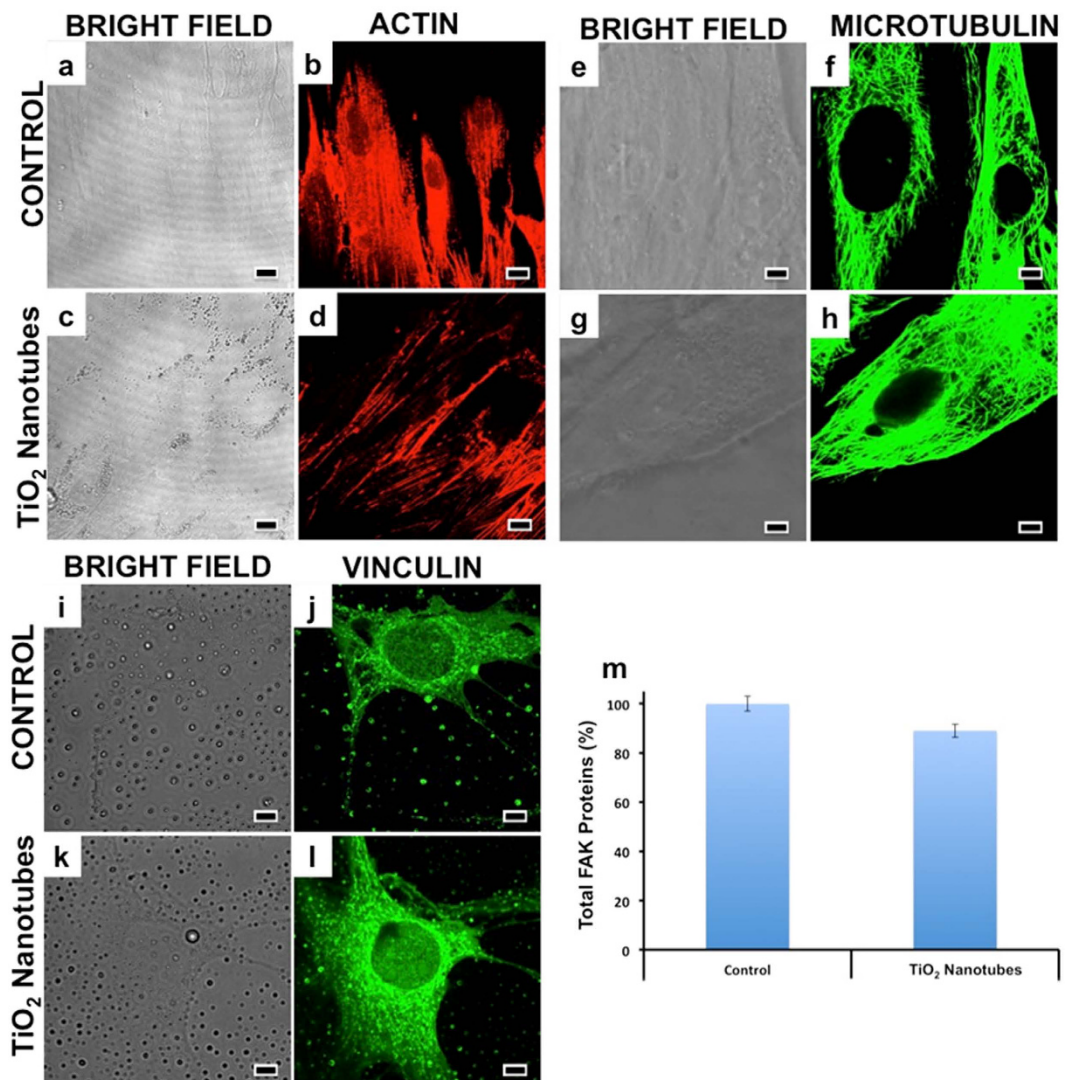


Figure 4. Cytoskeletal integrity analysis of the control and NTs treated group were performed with emphasis on actin, microtubulins and vinculin. With respect to the actin filaments, a slight reduction in the network of the fibres was observed with the NT group (d) when compared with the control (b). In the case of microtubulins the control (f) and test groups (h) exhibited comparable tubular network. The vinculin expression was found to be undisturbed in the treatment group (l) when compared to control (j). (Scale bars represent 10 μ m). Total FAK proteins were quantified with ELISA and their expression in control and treatment groups remained comparable (m). Overall, the cytoskeletal components, which form the basic backbone of a cell and are responsible for their structural integrity and cell-cell/cell-matrix interactions, remained unaffected by the TiO₂ NTs, with the exception of actin where a slight rearrangement of the fibers was observed.

condensation and double strand DNA breaks. When compared to the normal nuclear content (Fig. 6b), cells treated with NTs for 72 h displayed nuclear chromatin condensation and compromised plasma membrane permeability (Fig. 6d) suggesting cell death via an apoptotic mode. To analyze the secondary effects of ROS, immediate mediator of ROS-induced cell death mediated signaling, NF- κ B activation was profiled. As expected, nearly twice the increase in NF- κ B levels were noted when compared to controls (Fig. 6e). NF- κ B is considered as primary transcription factor of apoptosis that are expressed when cells are in oxidative distress. Their cytosolic expression increases immediately after an oxidative stress, and is transported to nucleus to induce apoptotic transcription leading to programmed cell death⁶⁸. A clear correlation between the ROS levels and NF- κ B expression could be made, which confirmed that the nuclear oxidative stress was the reason for observed genotoxic behavior.

To analyze whether chromosomal distortion occurred in the treatment groups, the cells were subjected to comet assay. A distorted chromosomal content, leads to tail-comet whereas the healthy chromosomal content appears spherical when subjected to comet electrophoresis. As expected, cells exposed to NTs exhibited nearly 7-fold increase in comet tail formation (Fig. 6f) again affirming the nuclear degeneration behavior of NTs. TiO₂ nanoparticles might damage DNA directly or indirectly via oxidative stress and/or inflammatory responses. Recent studies showed a direct chemical interaction between TiO₂ nanoparticles and DNA damage^{69,70}. However,

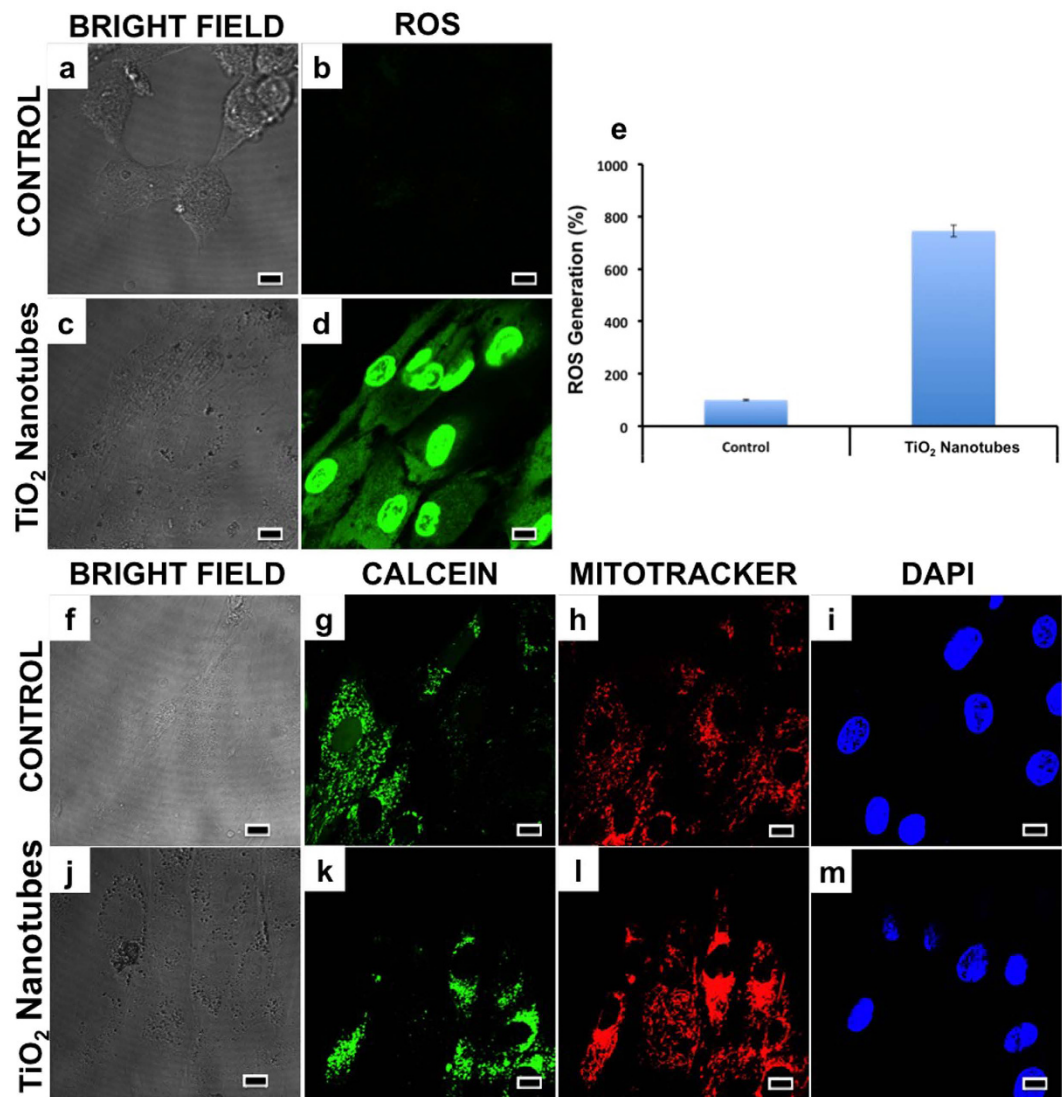


Figure 5. Mitochondrial integrity and condition were assayed with the ROS generation and transition pore formation tests. It was clearly evident that the NTs induced ROS production, especially nuclear ROS (d). The nuclear ROS in the treatment group was found to be increased by 7 fold than the control (e). The mitochondrial pore induction investigation revealed the absence of any distorted signals from the mitochondrial region (l) with discrete calcein signaling (k), indicative of a properly functioning mitochondrial system. (Scale bars represent 10 μm). It is evident from this assay that though the mitochondrial apparatus seems to be healthy and functioning properly, nuclear ROS is significantly enhanced on TiO₂ NTs exposure, which may be the precursor for numerous distortions in nuclear functioning.

other studies showed that TiO₂ nanoparticles could cause DNA damage through inflammation^{71,72} and/or ROS generation^{73,74}. We performed H2AX staining, that is indicative of DNA breaks. The treatment group cells exhibited numerous DNA breaks in the nuclear compartment that are indicative of spontaneous DNA damage due to NT exposure (Fig. 6k). It was evident that oxidative stress could be sensed by the nucleus and that ROS formation was directly generated by the nucleus. Increased ROS in the nuclear region due to NT exposure attacked the nuclear components leading to genotoxicity by inducing nuclear condensation and chromosomal distortion.

Conclusion

The results from our study indicated induction of ROS by NTs that in turn set off DNA damage and chromosomal aberrations, which are believed to be the primary factors resulting in cell cycle arrest. Cells resting at sub G₀ interface showed no significant death, indicating the involvement of an active DNA repair pathway. Cells with a robust repair mechanism in place could re-enter the cell cycle, while those with extensive irreparable damage could not repair the DNA effectively, consequently undergoing apoptosis. The NTs displayed the potential to cause toxicity to the cells as analyzed by the cyto- and genotoxicity parameters. Keeping in mind that the NTs were not surface modified with cyto-, biocompatible moieties as polyethylene glycol etc., it is imperative that the biological applications employing NTs should be given special attention and further studies must be conducted

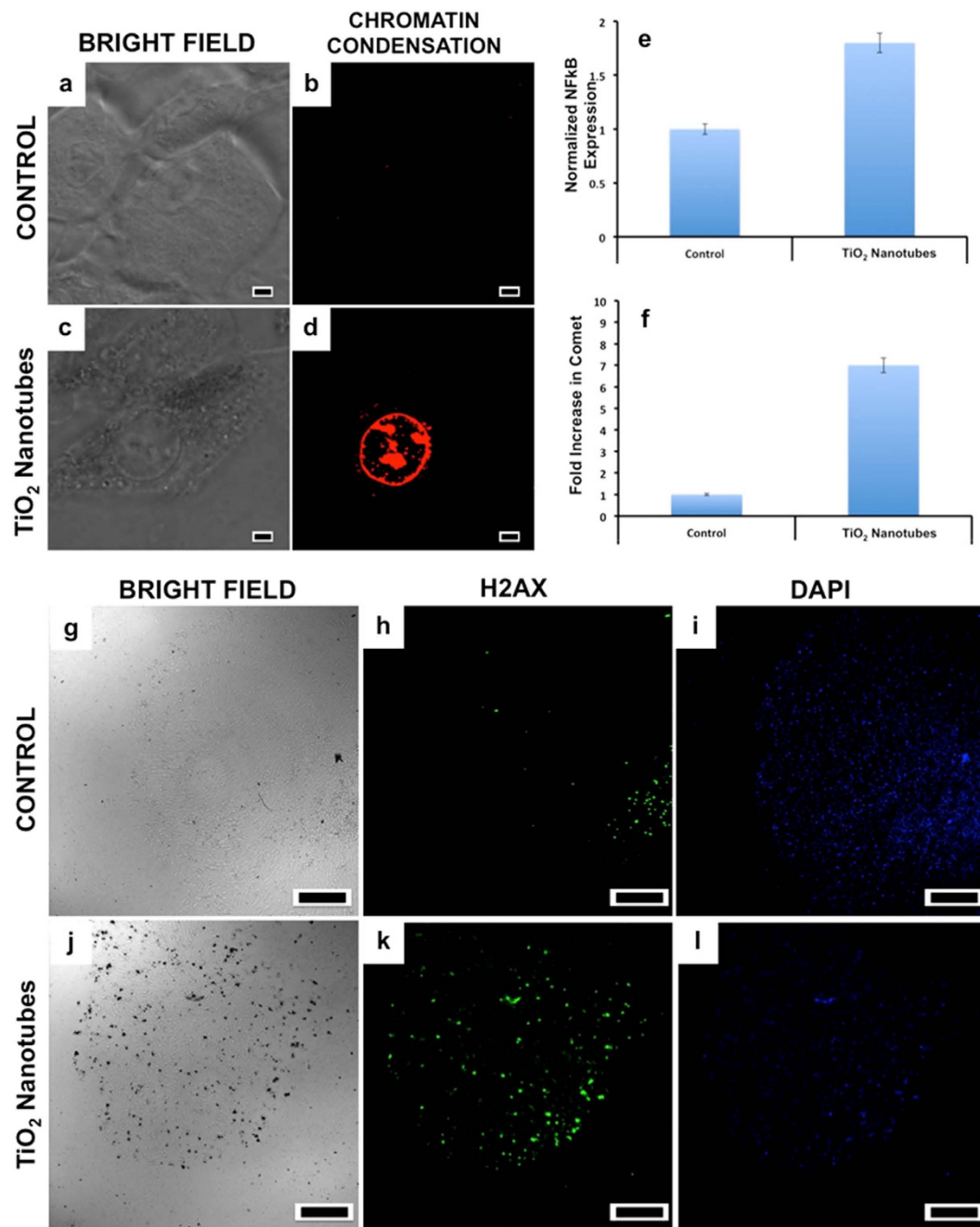


Figure 6. Chromatin condensation and DNA break studies were carried out to assess the condition of the nuclear set up of the control and NT treated cells. Prominent chromatin condensation and plasma membrane permeability (c,d) was recorded with the NTs treated group. (Scale bars represent 10 μ m). The NF- κ B expression was elevated in the treatment group when compared to control (e). Comet analysis confirmed significant increase in number of comet tails in treatment group (f). Consistent DNA breaks could also be observed with the H2AX test in the NTs group (k) when compared to the controls (h). (Scale bars represent 500 μ m). This nuclear condensation and DNA alteration study is correlative of the ROS induction previously observed.

in this field to achieve deeper understanding of NT toxicity. As mostly all the nanomaterials currently being examined for various applications including nanomedicine, pose toxicity *in vitro/in vivo*, and surface functionalization is mandatory, we believe that the TiO₂ NTs utilized in the present study could hold better performance once a biocompatible coating is rendered to them. Also, as the cause of cell death is proven to be ROS instigated genotoxicity, these TiO₂ nanotubes, after proper surface functionalization and with the assistance of cell-specific markers (antibodies/peptides) could be utilized as specific-cell killing tools, as in the case of anti-cancer therapies. For example, our current interest includes the utilization of such a properly functionalized and targeted TiO₂ nanotube to specifically induce ROS and genotoxic effects in cancer cells and kill them as such, negating the need for any chemo agent or external stimuli.

Materials and Methods

Titania nanotube synthesis. The titania nanotube array samples were fabricated by anodic oxidation of titanium (Ti) foils (0.25 mm thick, 99.7% pure, Sigma Aldrich) in a two-electrode cell consisting of a titanium foil anode and a platinum foil cathode immersed in an aqueous or organic electrolyte. The aqueous electrolyte consisted of 0.5 vol% HF in deionized (DI) water. The anodization of Ti foil at 10 V for 1 h in this electrolyte yielded nanotubes having morphology shown in Fig. 1a,b. The organic electrolyte was prepared by mixing EG with 0.7 vol% ammonium fluoride (NH₄F) and 50 vol% DI water. The nanotubes (Fig. 1c,d) were grown by anodizing Ti foil at 15 V for 1 h. The titania nanotube array samples prepared in these aqueous and organic electrolytes were then crystallized by heat treating respectively at 500 °C and 450 °C for 30 minutes in oxygen environment. The heat treated samples were anodized again in the respective electrolytes and voltages to detach the crystallized nanotubes from the metal substrate.

Cell culture details. Human Dermal Adult Fibroblasts (HDAF) were obtained from ATCC. The cells were maintained in T25 flasks using CSC complete medium kit (Cell Systems), and incubated in a 5% CO₂ incubator at 37 °C. The cells were sub-cultured every three days. Approximately 5000 cells were seeded into each well of 96 well plates. After attaining visual confluency, NTs were added at different concentrations (0.05 mg/mL– 1 mg/mL). Control group was devoid of NTs. After 72 h of incubation with NTs, cells were washed with PBS and 0.2 ml of respective medium was added. Cell viability was assayed with alamar blue in a 96 well plate reader (Multidetector microplate scanner, Dainippon Sumitomo Pharma). For other microplate assays, NTs at a concentration of 0.05 mg/mL were added to the cells and incubated for 72 h. Post 72 h, the cells were quantified for lactate dehydrogenase (LDH) release (Pierce LDH cytotoxicity kit), total cellular protein contents (Pierce BCA protein assay kit), total focal adhesion kinase (FAK) expression (FAK ELISA kit, Thermo Fisher), reactive oxygen species (ROS) generation (DCFH-DA Assay, Sigma) and nuclear factor- κ B (NF- κ B) expression (NF- κ B transcription factor assay kit, Thermo Fisher) according to the respective manufacturer's instructions.

For flow cytometry (JSAN cell sorter, Bay Bioscience) based cell cycle analysis, approximately 200,000 cells were seeded in 6 well plates and cultured for 24 h. NTs (0.05 mg/mL) were added to the cultures and incubated for 72 h. Post incubation, cells were washed in PBS and flow cytometry performed according to manufacturer's instructions (Click-iT EDU Alexa fluor 488 flow cytometry assay kit, Life technologies).

For all confocal (CLSM, Olympus IX 81 under DU897 mode; for blue, green and red excitations, wavelength 405, 488 and 561 were used respectively) experiments, approximately 50,000 cells were cultured in 35 mm glass base dishes (Iwaki) for 24 h. The cells were incubated with the NTs (0.05 mg/mL) for 72 h. Live/dead (Live/dead cell double staining kit, Sigma-Aldrich), EDU cell proliferation (Click-iT[®] Plus EdU, Life Technologies), Actin (Phalloidin rhodamine, Life technologies), Microtubulin (Tubulin tracker, Life technologies), ROS (Cell-ROX, Life technologies), Mitochondrial pore induction (Mitochondrial membrane transition pore assay, Life technologies), Chromatin condensation (Life technologies), DNA break (HCS DNA damage kit, Life technologies) assays were performed as per the respective manufacturer's instructions.

For comet assay, cells were grown until 80% confluency in T25 flasks. Treatment groups were exposed to 0.05 mg/mL of NTs whereas controls were devoid of any treatment. Post 72 h exposure, cells were collected and processed for comet assay as per manufacturer's instructions (Alkaline Comet, Trevigen). The comet formations were counted manually and were graphed.

For all cell culture experiments, the cells were washed thoroughly with PBS after incubation with the NTs for the specified time period to remove any unbound or free floating NTs, prior to observations.

Statistical analysis. All quantitative experiments were conducted with at least three independent experiments, each with triplicates. Statistical evaluation was performed using Origin Pro Software.

References

- Shvedova, A. A., Pietroiusti, A., Fadeel, B. & Kagan, V. E. Mechanisms of carbon nanotube-induced toxicity: focus on oxidative stress. *Toxicol. Appl. Pharm.* **261**, 121–133 (2012).
- Pojlak-Blazi, M., Jaganjac, M. & Zarkovic, N. Cell oxidative stress: risk of metal nanoparticles. *Handbook of Nanophysics: Nanomedicine and Nanorobotics*, CRC Press, New York, NY, USA, 1–17 (2010).
- Papavlassopoulos, H. *et al.* Toxicity of functional nano-micro zinc oxide tetrapods: impact of cell culture conditions, cellular age and material properties. *PLoS One*. **9**, e84983 (2014).
- Ju-Nam, Y. & Lead, J. R. Manufactured nanoparticles: an overview of their chemistry, interactions and potential environmental implications. *Sci. Tot. Environ.* **400**, 396–414 (2008).
- Li, N., Xia, T. & Nel, A. E. The role of oxidative stress in ambient particulate matter-induced lung diseases and its implications in the toxicity of engineered nanoparticles. *Free Radic. Biol. Med.* **44**, 1689–1699 (2008).
- Stone, V., Johnston, H. & Cli, M. J. D. Air pollution, ultra fine and nanoparticle toxicology: cellular and molecular interactions. *IEEE Trans. Nanobioscience*. **6**, 331–340 (2007).
- Johnston, H. J. *et al.* A review of the *in vivo* and *in vitro* toxicity of silver and gold particulates: particle attributes and biological mechanisms responsible for the observed toxicity. *Crit. Rev. Toxicol.* **40**, 328–346 (2010).
- Sotiriou, G. A. *et al.* A novel platform for pulmonary and cardiovascular toxicological characterization of inhaled engineered nanomaterials. *Nanotoxicology*. **6**, 680–690 (2012).
- Sadeghi, L., Yousefi Babadi, V. & Espanani, H. R. Toxic effects of the Fe₂O₃ nanoparticles on the liver and lung tissue. *Bratisl Lek Listy*. **116**, 373 – 378 (2015).
- Vandebriel, R. J. & De Jong, W. H. A review of mammalian toxicity of ZnO nanoparticles. *Nanotechnol. Sci. Appl.* **5**, 61–71 (2012).
- Han, D., Tian, Y., Zhang, T., Ren, G. & Yang Z. Nano-zinc oxide damages spatial cognition capability via over-enhanced long-term potentiation in hippocampus of Wistar rats. *Int. J. Nanomedicine*. **6**, 1453 –1461 (2011).
- Kim, Y.-R. *et al.* Toxicity of 100 nm zinc oxide nanoparticles: a report of 90-day repeated oral administration in Sprague Dawley rats. *Int. J. Nanomedicine*. **9**, 109–126 (2014).
- Kumari, M., Kumari, S. I. & Grover, P. Genotoxicity analysis of cerium oxide micro and nanoparticles in Wistar rats after 28 days of repeated oral administration. *Mutagenesis*. **29**, 467–479 (2014).

14. Morimoto, Y. *et al.* Pulmonary toxicity of well-dispersed cerium oxide nanoparticles following intratracheal instillation and inhalation. *J. Nanopart. Res.* **17**, 442 (2015).
15. Qin, P. *et al.* Stable and efficient perovskite solar cells based on titania nanotube arrays. *Small*. **11**, 5533–5539 (2015).
16. Wijeratne, A. B. *et al.* Phosphopeptide separation using radially aligned titania nanotubes on titanium wire. *ACS Appl. Mater. Interfaces*. **7**, 11155–11164 (2015).
17. Stern, S. T. & McNeil, S. E. Nanotechnology: safety concerns revisited. *Toxicol Sci.* **101**, 4–21 (2008).
18. Lewinski, N., Colvin, V. L. & Drezek, R. Cytotoxicity of nanoparticles. *Small*. **4**, 26–49 (2008).
19. Poulouse, A. C. *et al.* Characterizing the biocompatibility and tumor imaging capability of Cu₂S nanocrystals *in vivo*. *Nanoscale*. **7**, 13061–13074 (2015).
20. Helland, A., Wick, P., Koehler, A., Schmid, K. & Som, C. Reviewing the environmental and human health knowledge base of carbon nanotubes. *Environ. Health Perspect.* **115**, 1125–1131 (2007).
21. Lam, C. W., James, J. T., McCluskey, R. & Hunter R., L. Pulmonary toxicity of single-wall carbon nanotubes in mice 7 and 90 Days after Intratracheal Instillation. *Toxicol. Sci.* **77**, 126–134 (2004).
22. Warheit, D. B. *et al.* Comparative pulmonary toxicity assessment of single-wall carbon nanotubes in rats. *Toxicol. Sci.* **77**, 117–125 (2004).
23. Shvedova, A. A. *et al.* Exposure to carbon nanotube material: assessment of nanotube cytotoxicity using human keratinocyte cells. *J. Toxicol. Environ. Health A*. **66**, 1909–1926 (2003).
24. Maynard, A. D. *et al.* Exposure to carbon nanotube material: aerosol release during the handling of unrefined single-walled carbon nanotube material. *J. Toxicol. Environ. Health A*. **67**, 87–107 (2004).
25. Monteiro-Riviere, N. A., Nemanich, R. J., Inman, A. O., Wang, Y. Y. & Riviere, J. E. Multi-walled carbon nanotube interactions with human epidermal keratinocyte. *Toxicol. Lett.* **155**, 377–384 (2005).
26. Panessa-Warren, B. J., Warren, J. B., Wong, S. S. & Misewich, J. A. Biological cellular response to carbon nanoparticle toxicity. *J. Phys. Condens. Mater.* **18**, S2185–S2201 (2006).
27. van den Brule, S. *et al.* Nanometer-long Ge-imogolite nanotubes cause sustained lung inflammation and fibrosis in rats. *Part. Fibre Toxicol.* **11**, 67 (2014).
28. Silva, R. M. *et al.* Short versus long silver nanowires: a comparison of *in vivo* pulmonary effects post instillation. *Part. Fibre Toxicol.* **11**, 52 (2014).
29. Schinwald, A. & Donaldson, K. Use of back-scatter electron signals to visualise cell/nanowires interactions *in vitro* and *in vivo*; frustrated phagocytosis of long fibres in macrophages and compartmentalisation in mesothelial cells *in vivo*. *Part. Fibre Toxicol.* **9**, 34 (2012).
30. Roberts, J. R. *et al.* Pulmonary toxicity, distribution, and clearance of intratracheally instilled silicon nanowires in rats. *Journal of Nanomaterials* **2012**, 398302 (2012).
31. Rao, B. M., Torabi, A. & Varghese, O. K. Anodically grown functional oxide nanotubes and applications, MRS Communications, doi: <https://doi.org/10.1557/mrc.2016.46>.
32. Niinomi, M. Mechanical biocompatibilities of titanium alloys for biomedical applications. *J. Mech. Behav. Biomed. Mater.* **1**, 30–42 (2008).
33. Wang, K. The use of titanium for medical applications in the USA. *Mater. Sci. Eng. A*. **213**, 134–137 (1996).
34. Gong, D. *et al.* Titanium oxide nanotube arrays prepared by anodic oxidation. *J. Mater. Res.* **16**, 3331–3334 (2001).
35. Rani, S. *et al.* Synthesis and applications of electrochemically self-assembled titania nanotube arrays. *Phys. Chem. Chem. Phys.* **12**, 2780–2800 (2010).
36. Brahmi, H. *et al.* Thermal-structural relationship of individual titania nanotubes. *Nanoscale*. **7**, 19004–19011 (2015).
37. Popat, K. C., Leoni, L., Grimes, C. A. & Desai, T. A. Influence of engineered titania nanotubular surfaces on bone cells. *Biomaterials*. **28**, 3188–3197 (2007).
38. Bauer, S., Park, J., von der Mark, K. & Schmuki, P. Improved attachment of mesenchymal stem cells on super-hydrophobic TiO₂ nanotubes. *Acta. Biomater.* **4**, 1576–1582 (2008).
39. Park, J., Bauer, S., von der Mark, K. & Schmuki, P. Nanosize and vitality: TiO₂ nanotube diameter directs cell fate. *Nano Lett.* **7**, 1686–1691 (2007).
40. Bauer, S. *et al.* Size selective behavior of mesenchymal stem cells on ZrO₂ and TiO₂ nanotube array. *Integr. Biol.* **1**, 525–532 (2009).
41. Smith, C. M. *et al.* Engineering a titanium and polycaprolactone construct for a biocompatible interface between the body and artificial limb. *Tissue Eng. A*. **16**, 717–724 (2010).
42. Kang, N. V., Pendegrass, C., Marks, L. & Blunn, G. Osseocutaneous integration of an intraosseous transcutaneous amputation prosthesis implant used for reconstruction of a transhumeral amputee: case report. *J. Hand. Surg.* **35**, 1130–1134 (2010).
43. Tillander, J., Hagberg, K., Hagberg, L. & Bränemark, R. Osseointegrated titanium implants for limb prostheses attachments: infectious complications. *Clin. Orthop. Relat. Res.* **468**, 2781–2788 (2010).
44. Mooney, V., Predecki, P. K., Renning, J. & Gray, J. Skeletal extension of limb prosthetic attachments – Problems in tissue reaction. *J. Biomed. Mater. Res.* **5**, 143–159 (1971).
45. Winter, G. D. Transcutaneous implants: reactions of the skin-Implant interface. *J. Biomed. Mater. Res.* **8**, 99–113 (1974).
46. Varghese, O. K., Gong, D., Paulose, M., Grimes, C. A. & Dickey, E. C. Crystallization and high temperature structural stability of titanium oxide nanotube arrays. *J. Mater. Res.* **18**, 156–165 (2003).
47. Paulose, M., Shankar, K., Yoriya, S., Prakasam, H. E., Varghese, O. K., Mor, G. K., LaTempa, T. A., Fitzgerald, A. & Grimes, C. A. Anodic growth of highly ordered TiO₂ nanotube arrays to 134 μm in length. *J. Phys. Chem. B*. **110**, 16179–16184 (2006).
48. Horváth, L. *et al.* *In vitro* investigation of the cellular toxicity of boron nitride nanotubes. *ACS Nano*. **5**, 3800–3810 (2011).
49. Huang, Y. Y. & Terentjev, E. M. Dispersion of carbon nanotubes: mixing, sonication, stabilization, and composite properties. *Polymers*. **4**, 275–295 (2012).
50. Pagani, G., Green, M. J., Poulin, P. & Pasquali, M. Competing mechanisms and scaling laws for carbon nanotube scission by ultrasonication. *PNAS*. **109**, 11599–11604 (2012).
51. Love, S. A., Maurer-Jones, M. A., Thompson, J. W., Lin, Y. S. & Haynes, C. L. Assessing nanoparticle toxicity. *Annu. Rev. Anal. Chem.* **5**, 181–205 (2012).
52. Maurer-Jones, M. A., Lin, Y. S. & Haynes, C. L. Functional assessment of metal oxide nanoparticle toxicity in immune cells. *Am. Chem. Soc. Nano*. **4**, 3363–3373 (2010).
53. Ji, Z. *et al.* Dispersion and stability optimization of TiO₂ nanoparticles in cell culture media. *Environ. Sci. Technol.* **44**, 7309–7314 (2010).
54. Tedja, R., Marquis, C., Lim, M. & Amal, R. Biological impacts of TiO₂ on human lung cell lines A549 and H1299: particle size distribution effects. *J. Nano Res.* **13**, 3801–3813 (2011).
55. Tilly, T. B., Kerr, L. L., Braydich-Stolle, L. K., Schalger, J. J. & Hussain, A. M. Dispersions of geometric TiO₂ nanomaterials and their toxicity to RPMI 2650 nasal epithelial cells. *J. Nanopart. Res.* **16**, 2695 (2014).
56. Chan, F. K., Moriwaki, K. & De Rosa, M. J. Detection of necrosis by release of lactate dehydrogenase activity. *Methods Mol. Biol.* **979**, 65–70 (2013).
57. Brown, G. C. Total cell protein concentration as an evolutionary constraint on the metabolic control distribution in cells. *J. Theor. Biol.* **153**, 195–203 (1991).

58. Riss, T. L., Moravec, R. A. & Niles, A. L. Cytotoxicity testing: measuring viable cells, dead cells, and detecting mechanism of cell death. *Methods Mol. Biol.* **740**, 103–114 (2011).
59. Nunez, R., Sancho-Martinez, Novoa, J. M. L. & Lopez-Hernandez, F. J. Apoptotic volume decrease as a geometric determinant for cell dismantling into apoptotic bodies. *Cell Death. Differ.* **17**, 1665–1671 (2010).
60. Ono, S. Mechanism of depolymerization and severing of actin filaments and its significance in cytoskeletal dynamics. *Int. Rev. Cytol.* **258**, 1–82 (2007).
61. Vale, R. D. The molecular motor toolbox for intracellular transport. *Cell.* **112**, 467–480 (2003).
62. Carisey, A. & Ballestrem, C. Vinculin, an adapter protein in control of cell adhesion signaling. *Eur. J. Cell. Biol.* **90**, 157–163 (2011).
63. Grashoff, C. *et al.* Measuring mechanical tension across vinculin reveals regulation of focal adhesion dynamics. *Nature.* **466**, 263–266 (2010).
64. Holt, B. D. *et al.* Carbon nanotubes reorganize actin structures in cells and *ex vivo*. *ACS Nano.* **4**, 4872–4878 (2010).
65. Huang, K. T. *et al.* Titanium nanoparticle inhalation induces renal fibrosis in mice via an oxidative stress upregulated transforming growth factor- β pathway. *Chem. Res. Toxicol.* **28**, 354–364 (2015).
66. Mohamed, M. S. *et al.* Cytological and subcellular response of cells exposed to the type-1 RIP curcun and its hemocompatibility analysis. *Sci. Rep.* **4**, 5747 (2014).
67. Wang, Y. *et al.* Direct imaging of titania nanotubes located in mouse neural stem cell nuclei. *Nano Res.* **2**, 543–552 (2009).
68. Wan, F. & Leonardo, M. J. The nuclear signaling of NF- κ B: current knowledge, new insights, and future perspectives. *Cell Res.* **20**, 24–33 (2010).
69. Li, S. *et al.* Impact and mechanism of TiO₂ nanoparticles on DNA synthesis *in vitro*. *Sci. Chin. Ser. B Chem.* **51**, 367–372 (2008).
70. Zhu, R. R., Wang, S. L., Zhang, R., Sun, X. Y. & Yao, S. D. A novel toxicological evaluation of TiO₂ nanoparticles on DNA structure. *Chin. J. Chem.* **25**, 958–961 (2007).
71. Chen, H. W. *et al.* Titanium dioxide nanoparticles induce emphysema-like lung injury in mice. *FASEB J.* **20**, 2393–2395 (2006).
72. De Haar, C., Hassing, I., Bol, M., Bleumink, R. & Pieters R. Ultrafine but not fine particulate matter causes airway inflammation and allergic airway sensitization to co-administered antigen in mice. *Clin. Exp. Allergy.* **36**, 1469–1479 (2006).
73. Gurr, J. R., Wang, A. S., Chen, C. H. & Jan, K. Y. Ultrafine titanium dioxide particles in the absence of photoactivation can induce oxidative damage to human bronchial epithelial cells. *Toxicol.* **213**, 66–73 (2005).
74. Veranth, J. M., Kaser, E. G., Veranth, M. M., Koch, M. & Yost, G. S. Cytokine responses of human lung cells (BEAS-2B) treated with micron-sized and nanoparticles of metal oxides compared to soil dusts. *Part. Fibre. Toxicol.* **4**, 2 (2007).

Acknowledgements

A part of this study was supported by a grant for the program of strategic research foundation at private universities S1101017, organized by the Ministry of Education, Culture, Sports, Science and Technology (MEXT), Japan since April 2012.

Author Contributions

M.S.M., D.S.K. and O.K.V. conceived and designed the work; A.T. and M.P. performed the synthesis of NTs. The characterizations were performed by M.S.M. and M.P. M.S.M. conducted and analyzed *in vitro* cellular investigations. M.S.M., A.T., M.P., O.K.V. and D.S.K. critically analyzed the results. M.S.M. and O.K.V. wrote the manuscript with input from co-authors.

Additional Information

Supplementary information accompanies this paper at <http://www.nature.com/srep>

Competing financial interests: The authors declare no competing financial interests.

How to cite this article: Mohamed, M. S. *et al.* Anodically Grown Titania Nanotube Induced Cytotoxicity has Genotoxic Origins. *Sci. Rep.* **7**, 41844; doi: 10.1038/srep41844 (2017).

Publisher's note: Springer Nature remains neutral with regard to jurisdictional claims in published maps and institutional affiliations.



This work is licensed under a Creative Commons Attribution 4.0 International License. The images or other third party material in this article are included in the article's Creative Commons license, unless indicated otherwise in the credit line; if the material is not included under the Creative Commons license, users will need to obtain permission from the license holder to reproduce the material. To view a copy of this license, visit <http://creativecommons.org/licenses/by/4.0/>

© The Author(s) 2017